INTERNATIONAL JOURNAL OF CLIMATOLOGY

*Int. J. Climatol.* **25**: 881–894 (2005)

Published online in Wiley InterScience (www.interscience.wiley.com). DOI: 10.1002/joc.1170

# A 1° MONTHLY GRIDDED SEA-SURFACE TEMPERATURE DATASET COMPILED FROM ICOADS FROM 1850 TO 2002 AND NORTHERN HEMISPHERE FRONTAL VARIABILITY

Shoshiro MINOBE and Atsushi MAEDA

*Division of Earth and Planetary Sciences, Graduate School of Science, Hokkaido University, Sapporo, Japan*

*Received 4 May 2004*

*Revised 20 November 2004*

*Accepted 2 December 2004*

## ABSTRACT

Using surface marine data collected in International Comprehensive Ocean Atmosphere Data Set (ICOADS) release 2.1, a gridded SST dataset on a monthly, 1°×1° grid is produced from 1850 to 2002. Some unrealistic features, which are commonly found in the gridded SSTs of ICOADS, are removed by a subjective quality control. Based on the gridded SST data, SST variability associated with the oceanic fronts is investigated for the North Atlantic and North Pacific.

Year-to-year SST variability in the North Atlantic is prominent along the climatological Gulf Stream Extension (GSE) in winter and spring. This correspondence is better captured in the present SST dataset than in several widely used datasets. GSE mean SST exhibits multidecadal variability similar to the Atlantic Multidecadal Oscillation represented by mean SSTs over the North Atlantic.

Year-to-year SST variability in the North Pacific in winter and spring seasons is strong along SubPolar Front (SAF), and also in SubTropical Front (STF) with weaker amplitudes in the latter. In particular, just east of Japan, Kuroshio extension appears to be a core of strong variability. Winter and spring averaged SAF and STF exhibit prominent decadal warmings in the 1940s, i.e., these fronts may be the two of action centers for the 1940s climate regime shift as well as the previously reported 1970s shift. The warming anomalies around SAF associated with the 1940s shift distributed more broadly than those with the 1970s shift, and have maximal amplitudes around Japan.

KEY WORDS: SST; ICOADS gridded dataset; frontal variability; decadal variability

## 1. INTRODUCTION

Sea surface temperature (SST) is a fundamental parameter for discussion of climate variability. SST observations, except for satellite observations, randomly distribute in space and time and are difficult to be treated directly by a wide range of researchers. Therefore, tractable gridded SST datasets are quite important for climate researches.

In general, SST datasets available through the 20th century can be classified into two categories, i.e., little or not interpolated SST datasets and heavily interpolated SST datasets. A couple of examples of the former are UK Meteorological Office Historical SST data set (MOHSST) on a monthly 5°×5° grid (Parker et al. 1995), and gridded SSTs of ICOADS on a monthly 2°×2° grid. ICOADS (Worley et al. 2004) is the successor of Comprehensive Ocean-Atmosphere Data Set (COADS) (Woodruff et al. 1987). Examples of heavily interpolated SST datasets are the Hadley Centre Sea Ice and Sea Surface Temperature data set (HadISST) from the UK Met Office (Rayner et al, 2003), Reynolds reconstructed SST data from National Centers for Environmental Prediction (NCEP) (Smith and Reynolds, 2004), and SST data produced by Kaplan et al (1997). These two categories of SST datasets have different advantages and disadvantages. The heavily interpolated SST datasets can have complete spatial and temporal coverage, which is required to force atmospheric climate models for studies of climate variability and predictability, and to assess the SST climatology of coupled climate models. The interpolation, however, can include false gridded values. The SST datasets without interpolations do not involve artificial data, but have substantial data-missing areas especially in the 19th and the early 20th centuries. For recent decades, satellite observations allow global coverage of SST datasets without heavy interpolations (e.g., Reynolds and Smith, 1994).

In the present paper, we produce a gridded SST anomaly dataset on a monthly 1°×1° grid without any spatial smoothing nor spatial interpolation for anomaly field; this dataset has the highest effective resolution compared with the aforementioned other SST datasets. As an application of this SST dataset, we analyze the variability of Gulf Stream Extension (GSE) in the North Atlantic, and SubArctic Front (SAF) and SubTropical Front (STF) in the North Pacific.

The rest of the present paper is organized as follows. In section 2, method of gridding is described. In section 3, overall features of global SST fields are explained. The GSE variability described in section 4, and variability of SAF and STF are examined in section 5. Summary and discussion are presented in section 6.

## 2. OBSERVATIONAL DATA AND GRIDDING METHOD

The SST observations used for this dataset were taken from ICOADS release 2.1 (Worley et al. 2004). ICOADS includes recent digitalization of Japanese Kobe collection for the observations before 1931, and the data coverage has been substantially improved mainly in the Pacific Ocean (Manabe 1999). Also, Ishii et al. (this issue) produced monthly 1°×1° SST anomaly dataset using ICOADS (release 2.0) and Kobe collection. They employed an Optimal Interpolation technique and also interpolations based on EOFs, and hence their dataset is

heavily interpolated.

We gridded global SST observations from 1850 to 2002. As will be explained in the next subsection, some erroneous data were removed by a subjective quality control. The data passed the subjective assessments are processed for the objective quality control and gridding.

### *2.1. Subjective quality control*

Widely used objective quality controls based on a standard deviation of anomalies may be insufficient to remove an unrealistic data, when the population ratio of the unrealistic data is large in a certain region. An example of unrealistic feature is a couple of squares of the SST anomalies over the central North Pacific apparent in the gridded version of ICOADS available since 1960 on a 1°×1° grid (Fig. 1). We obtain similar feature, when we produce SST dataset without a subjective quality control. The problem of the unrealistic SSTs over the central North Pacific in ICOADS was known by some researchers (personal communication, Dr. T. Mitchell), but the source of the problematic data was not previously documented.

In order to identify the possible sources of the unrealistic SSTs at specific locations and times, we plotted a histogram, a temperature-time scattered diagram, and several other kinds of plots for each of major deck numbers. A deck number is a code number that indicates the source country and organization that obtained the data. From a visual inspection of these plots, we determine how to remove the data that can be the source of the unrealistic feature of the gridded data.

In order to illustrate how we determine the removal scheme, we plot histogram of SST data of deck number 732 and SST data of other deck number for the aforementioned unrealistic squares over the central North Pacific (40°–45°N, 175°–170°W and 165°–160°W) (Fig. 2). The deck number 732 means Russian marine meteorological data set received at National Center for Atmospheric Research (NCAR). It is apparent that the probability distribution function for the deck number 732 is significantly different from that for other deck numbers. The SSTs of deck number 732 are generally colder than the SSTs of other deck numbers. The number of SST observations of deck number 732 is the largest (40%) in this region, with the second largest observation number of 14%; the ratio of the deck number 732 is too large to be removed by an objective quality control. We suspect that the location of a substantial portion of observations with deck number 732 may be wrong, because the vestige of similar unrealistic feature is also seen in sea-level pressures (SLPs). The doubtful distribution of the deck number 732 is observed only before 1975, and the data after 1976 are likely to be normal.

We also found several other unrealistic observations, and removed them. Observations removed by the subjective quality control are summarized in table 1. Some data listed here can be removed by an objective quality control, but we conservatively removed these apparently unrealistic data subjectively before the objective quality control. The present crude scheme of detection and removal of doubtful observations is useful for the purpose of this study, in which only SST data are gridded. However, it may be insufficient for a more general use. In future, it is desirable to detect doubtful data objectively by using a statistical approach, such as a statistical test of difference of distributions between two groups (e.g., different deck numbers).

### *2.2. Objective quality control and gridding*

The objective quality control and gridding are conducted as follows. First, we removed the data that are

colder -2°C or warmer than 37°C, and the data over land. We temporally calculated the SST climatology for every five days on a 1°×1° grid for the period 1950–2000[1]. When a monthly climatology value deviates from the annual mean climatology more than three standard deviations, the monthly climatology was replaced by the missing value. The climatology further smoothed by a 5-point median smoother temporally and zonally. We used these smoothing, because erroneous climatology can yields false anomalies associated with the spatial and temporal changes of observation locations. Since grid interval of data for which smoothing was applied is high spatially (1°) and temporally (5 day), this moderate smoothing does not obscure major frontal structures as described below. We used the 51-yr long base period for calculating climatology in order to suppress noises in the estimated climatology.

The resultant 5-day climatology is interpolated to a 1-day interval using the first four components of sinusoidal functions (annual, semiannual, 4-month, and 3-month components). Anomalies of respective observations are calculated using bi-linear spatial interpolation of daily climatology. An anomaly that has a larger amplitude than the 2.5-standard deviation of the anomalies at each grid and month are removed from further analyses. Then, the calculation of climatology and the quality control for the anomalies are repeated. The quality-controlled anomalies are gridded by using simple averaging in monthly 1°×1° bin. Neither spatial interpolation nor spatial smoothing is applied to the anomaly field.

The bucket correction of Folland and Parker (1995) are applied to the gridded SST anomalies by interpolating their 5°×5° correction values onto the 1°×1° grid. Their correction method assumes that before 1941 all SSTs were measured by buckets. However, recently added SST data of deck numbers 705, 706 and 707 have 80% of SST data measured via engine intake. Thus, for consistency, we removed these data also subjectively before the objective quality control (Table 1). We compared the corrected SST anomalies with the SST data of the World Ocean Database 2001 for data rich region around Japan, where correction values are the largest, and did not find substantial differences. The SST dataset produced in this study consists of the corrected SST anomalies.

## 3. OVERALL FEATURES OF SST ANOMALIES

Figure 3 shows a comparison of globally averaged monthly temperature anomalies of the present SST, HadiSST, and MOHSST between 60°S–70°N during the period 1880–2002. Overall features such as warming in the early 20th century and after 1970 are common in all datasets with comparable magnitude. A notable difference is strong cold anomalies from 1939 to 1941 in the present SST, which are not found neither in the HadiSST nor MOHSST. To identify the sources of the difference we need further investigations.

Figure 4 shows standard deviations of monthly 1°×1° SST anomalies during the 20th century. The standard deviations in mid- and high-latitudes are strong along the oceanic fronts such as the GSE in the North Atlantic

[1] We also examined quality control using climatology before 1950 and after that, but major conclusions of the present paper unchanged.

and SAF (around 40°N) in the North Pacific. Also, strong standard deviations south of Africa and east of South America are associated with climatological frontal structures. The SST variability over the North Atlantic and the North Pacific will be examined more closely in the following sections.

## 4. GULF STREAM EXTENSION

The strong standard deviation along the GSE in the North Atlantic is worth examining further. The GSE corresponded to the amplitude maxima of the first mode of SSTs in the North Atlantic (Deser and Blackmon 1993). Moreover, whether the GSE variability significantly influences the atmosphere (Ratcliffe and Murray 1970; Palmer and Sun 1985; Joyce et al. 2000; Wu and Rodwell 2003) or not (Frankignoul et al. 2001) is an interesting question with respect to the air-sea interaction in the North Atlantic.

Maps of standard deviations in each month indicate that the variability is stronger from December to May, but weaker from June to November (not shown). Consistently, winter-spring (December to May) averaged SST anomalies indicate strong variability along the climatological mean SST gradient corresponding to the mean GSE (Fig. 5). We also examined standard deviation map of detrended data of winter-spring SSTs, but the differences in standard deviation between the raw and detrended data are quite small; the pattern correlation is 0.98 and domain-mean standard deviations for the detrended data are smaller only by 3.4% than that for the raw data.

We compare standard deviations of winter-spring mean SST anomalies of other widely used long-term SST datasets, i.e., HadISST, ICOADS, and MOHSST, whose spatial grid intervals are 1°, 2° and 5°, respectively (Fig. 6). For consistency, we applied bucket SST correction of Folland and Parker (1995) to the ICOADS SSTs. The other two SST datasets were already corrected by the original providers. The present SST dataset depicts more strongly GSE-trapped SST variability than any of the other datasets. HadISST is likely to underestimate the SST variability, and the GSE-related high variability is somewhat broaden. The reason of the underestimation is that a smoothing was applied throughout the data set, and intrinsic resolution is lower before 1949 (personal communication, Dr. C. K. Folland). Amplitudes of ICOADS are nearly as strong as the present product, but strong variability along the GSE is less well separated from coastal variability. The 5° grid interval of MOHSST is apparently too coarse to distinguish the coastal variability and GSE variability. Consequently, the present SST product seems to capture the year-to-year GSE variability during the 20th century most successfully.

We calculate averaged winter-spring mean SST over grids whose standard deviation are larger than 1.3°C to the east of 75°W and south of 48°N ignoring coastal grids, and call it GSE mean SST (see Fig. 5 for which grids are used). The GSE mean SST indicates prominent multidecadal variability in addition to interannual variability (Fig. 7). This suggests that the GSE shifted its position on a multidecadal timescale, because the dominant variability of the year-to-year GSE is lateral shift (Joyce et al., 2000; Frankignoul et al. 2001). The multidecadal variability is generally consistent with the leading EOF mode of North Atlantic SSTs by Deser and Blackmon (1993). Recently, the dominant multidecadal variability over the North Atlantic is sometimes called the Atlantic Multidecadal Oscillation (AMO) (Enfield et al., 2001). Enfield et al. (2001) defined an AMO index as a time series of area-averaged SST anomaly over the North Atlantic. The AMO-like pattern was also shown by Folland et al (1986), who reported that this SST pattern is closely related to decadal variations in Sahel rainfall. Figure 7 also shows the winter-spring AMO time series based on the present SST dataset, indicating the

close linkage between the AMO and GSE SST. Actually, if we calculate regression coefficients of SSTs onto the AMO index, the highest regressions are observed along the GSE (not shown).

## 5. SUB-ARCTIC FRONT AND SUB-TROPICAL FRONT IN THE NORTH PACIFIC

In parallel to the analysis of the North Atlantic, we calculated standard deviation of SST anomalies averaged over the winter and spring seasons combined (December–May) for the North Pacific (Fig. 8). To the east of Japan, it is evident that strong standard deviations have two cores along the Kuroshio extension (KE) (35°N) and Oyashio Front (OF) (40°N). Also, around 40°N, 170°E, another cluster of strong standard deviation is observed. Around this location the northern branch of the Kuroshio bifurcation front merges with the Oyashio Front (Mizuno and White 1983). Combined with these systems, a broad band of strong mean SST gradients accompanied by large standard deviations around 40°N is called SAF (Nakamura et al. 1997) or Kuroshio-Oyashio Extension (Seager et al. 2001; Schneider et al. 2002) in climate researches. Weaker but sizable standard deviations associated with STF are observed from 25°–35°N to the east of the dateline (180°–140°W) and around 25°N to the west of it.

Figure 9 shows standard deviation of winter-spring SST anomalies based on the other SST datasets. Again, detailed spatial structures, i.e., two cores associated with the KE and OF, are smoothed out in HadiSST and MOHSST. The two-core structure is barely captured by the ICOADS, but the other maximum around the merging region of the OF and the northern branch of the Kuroshio bifurcation front is absent. In addition, in these SST datasets, it is difficult to see that the subtropical front has the strong standard deviations than those to the north and to the south.

The SAF and STF are interesting in terms of decadal climate variability and climatic regime shifts in the North Pacific. A number of papers investigated the North Pacific climatic regime shift occurred in the 1970s (e.g., Yamada and Nitta 1989; Trenberth 1990). Similar climatic shifts occurred also in the 1920s and 1940s (Minobe 1997; Mantua et al. 1997), and corresponding oscillatory variability in the ocean and atmosphere is called the Pacific (inter-)Decadal Oscillation (PDO) by Mantua et al. (1997). Minobe (1999; 2000) suggested that these three climatic regime shifts are marked by simultaneous phase reversals of the bi-decadal (about 20-yr) oscillation and pentadecadal (50–70 yr) oscillation. An interesting feature of the 1970s regime shift is that the SST difference before and after the shift has two action centers corresponding to the SAF and STF (Nakamura et al. 1997). Nakamura et al. (1997) suggested that the SAF variability is not related to the tropical changes, but STF has a close linkage with the tropics. Therefore, it is an interesting question what occurred for SAF and STF associated with the 1920s and 1940s regime shifts. However, the available grids are sparse over the North Pacific in the beginning of the 20th century, and hence we focus our attention to the 1940s regime shift.

Figure 10 shows the winter-spring (December–May) SST difference between two successive epochs separated by the regime shifts in the 1970s and 1940s. The SST difference for the 1970s regime shift is consistent with the pronounced cooling centered in the SAF (around 40°N) and STF (around 33°N) as documented by Nakamura et al. (1997). Also, the SST changes for the 1940s regime shift exhibit the two action centers associated with the SAF and STF, though STF change is weaker than the SAF change. The SST difference for the 1940s shift has larger amplitudes in SAF especially around Japan, consistent with SST analysis over the Pacific Ocean by Deser et al. (2004) and air-temperature analysis in Japan by Yamamoto et al. (1986).

Similar SST difference map is also calculated using 2°×2° ICOADS data (not shown). The signatures of SST warming appeared as less-prominently trapped by SAF and STF in the ICOADS SSTs than the present SSTs, partly due to the vestiges of unrealistic squares over the central North Pacific shown in Fig. 1.

Figure 11 shows the time series of SAF and STF since 1915; Before 1915, the number of observations are likely to be too small to confidently determine the SST anomalies of SAF and STF. Also, from 1942 to 1948, the number of observations was quite small associated with the World War II. However, warming in SAF and STF is prominent between 1915–1941 and 1949–1976. Therefore, combined with Fig. 10, the present result indicates that both SAF and STF warmed compared epochs before and after the 1940s regime shift. Due to the small number observations during the World War II, it is difficult to determine whether the apparent different timing of the SAF and STF warming is real or not. Although previous studies suggested that another climatic regime shift occurred in the mid 1920s in opposing polarity to the 1940s shift (Minobe 1997; Mantua et al. 1997), the SAF and STF time series do not show a prominent signature in the 1920s.

STF exhibited a rapid warming at 1999, consistent with basin-wide 1998/99 changes (Minobe 2002). On the other hand, SAF roughly returned to pre-1977 condition around 1990, and did not show substantial change in 1998/99. The nature of the 1998/99 change is under debate; A key question is whether this is another regime shift or not (e.g., Chavez et al. 2003). Minobe (2002) noted that the 1998/99 change is associated with the East Pacific pattern, characterized by a meridional dipole SLPs over the eastern North Pacific, while the other three shifts in the 1920s, 1940s and 1970s are more closely related to the Aleutian low strength changes. Consistently, Bond et al. (2003) showed that the 1998/99 change is associated with the SST second EOF mode in the North Pacific, but the 1970s shift is related to the first mode.

## 6. SUMMARY AND DISCUSSION

A gridded dataset of SST anomalies on a monthly 1°×1° grid is produced using SST observations collected in ICOADS release 2.1 without spatial interpolation and spatial smoothing. Unrealistic observations, which influenced the gridded data of ICOADS, were removed subjectively. As an application of the present SST dataset, GSE in the North Atlantic, and SAF and STF in the North Pacific are examined.

The strong variability associated with the GSE in the winter-spring SSTs is the most apparent in the present dataset than in the other widely used SST datasets, i.e., HadISST, ICOADS, and MOHSST. The GSE mean SST indicates multidecadal variability, and GSE is the strongest part of the Atlantic Multidecadal Oscillation.

In the North Pacific, strong SST variability is observed over SAF, with secondary amplitudes in STF. Just to the east of Japan, Kuroshio extension (35°N) and Oyashio Front (40°N) marked two cores of variability. The SAF and STF were the action centers of the SST warming associated with the climatic regime shift in the 1940s, as well as the cooling in the 1970s shift, consistent with the study by Nakamura et al. (1997) for the 1970s shift. However, the SST change associated with the 1940s shift exhibits broader changes around SAF than the 1970s shift, and were centered in Japan consistent with the strong warming signal in air-temperatures in Japan (Yamamoto et al. 1986).

Although we focused on the North Pacific, recent studies showed that Pacific decadal variability and two regime shifts in the 1940s and 1970s involve the southern hemisphere. Zhang et al. (1997) and Garreaud and Battisti (1999) showed that ENSO-like decadal variability, which is closely associated with the PDO (Mantua et

al., 1997), has a meridionally symmetric pattern with respect to the equator. Consistently, Folland et al. (1999; 2002) reported that the time series for a meridionally symmetric pattern, called Interdecadal Pacific Oscillation (IPO), highly resembles the PDO index. The IPO is obtained as a third EOF of low-pass filtered (period > 13-yr) global SSTs. Also, Linsley et al. (2004) showed that the IPO was well captured by South Pacific coral since 1880, though coral records seem to exhibit weaker multidecadal variability than those found in the IPO and PDO. Thus, the decadal SAF and STF variability may be viewed as regional manifestation of pan-Pacific decadal variability. It seems equally conceivable that the frontal variability plays an active role in the atmospheric variability (e.g., Nakamura et al. 1997; Tanimoto et al. 2003). For a better understanding of the roles of the oceanic fronts, further investigations are necessary.

No spatial interpolation and spatial smoothing in the present SST dataset ensures a high effective spatial resolution, but inevitably results in noisy monthly SST field. Thus, it may not be a good idea to show a SST snapshot at a certain month using this data. However, when we want to know the detailed spatial structures of averaged values (e.g., long-term means or GSE mean) or statistics (e.g., standard deviation), the present dataset can provide useful information that cannot be adequately obtained in other SST datasets.

## ACKNOWLEDGEMENTS

I thank to Dr. Woodruff and Ms. Manabe for encouraging to submit this paper, to Dr. Folland and an anonymous reviewer for their fruitful comments. This study was supported by grant-in-aid for scientific research (kaken-hi No. 15540417) and by 21st century center of excellence program on “Neo-Science of Natural History” (leader Prof. H. Okada) both from the Ministry of Education, Culture, Sports, Science and Technology, Japan.

## REFERENCES

Bond, N. A., J. E. Overland, M. Spillane, and P. Stabeno, 2003: Recent shifts in the state of the North Pacific. *Geophys. Res. Lett*., 30, 2183, doi:10.1029/2003GL018597.

Chavez, F. P., J., Ryan, S. E. Lluch-Cota, and C., M. Niquen, 2003: From anchovies to sardines and back: multidecadal change in the Pacific Ocean. *Science*, 299, 217-221.

Deser, C., and M. L. Blackmon, 1993: Surface Climate Variations over the North Atlantic Ocean during Winter: 1900-1989 *J. Climate*, **6**, 1743-1753.

Deser, C., A. S. Phillips, and J. W. Hurrell, 2004: Pacific Interdecadal Climate Variability: Linkages between the Tropics and North Pacific during boreal winter since 1900. *J. Climate*, **17**, 3109–3124.

Enfield D. B., A. M. Mestas-Nuñez and P. J. Timble, 2001: The Atlantic multidecadal oscillation and its relation to rainfall and river flows in the continental U.S. *Geophys. Res. Lett.*, **28**, 2077-2080, 2001.

Folland, C.K**.**, Parker, D.E. and T.N. Palmer, 1986: Sahel rainfall and worldwide sea temperatures 1901-85. *Nature*, **320,** 602-607.

Folland, C.K., Parker, D.E., Colman, A. and R. Washington, 1999: Large scale modes of ocean surface temperature since the late nineteenth century. Chapter 4, pp73-102 of *Beyond El Nino: Decadal and Interdecadal Climate Variability.* Ed: A. Navarra. Springer-Verlag, Berlin, pp 374.

Folland, C.K., J.A. Renwick, M.J. Salinger and A.B. Mullan, 2002: Relative influences of the Interdecadal

Pacific Oscillation and ENSO on the South Pacific Convergence Zone. *Geophys. Res. Lett.*, **29**, 10.1029/2001GL014201.

Folland, C. K. and D. E. Parker, 1995: Correction of instrumental biases in historical sea surface temperature data. *Q. J. R. Meteorol. Soc.*, **121**, 319–367.

Frankignoul, C., G.. D. Coëtlogon, T. M. Joyce, and S. Dong, 2001: Gulf stream variability and ocean-atmosphere interaction. *J. Climate,* **31**, 3516–3529.

Garreaud R. D., and D. S. Battisti, 1999: Interannual (ENSO) and interdecadal (ENSO-like) variability in the Southern Hemisphere tropospheric circulation. *J. Climate*, **12**, 2113-2123.

Ishii, M., A. Shouji, S. Sugimoto, and T. Matsumoto: Objective analyses of SST and marine meteorological variables for the 20th century using ICOADS and the Kobe collection. Int. J. Climatol. in press.

Kaplan, A., Y. Kushnir, M. Cane and B. Blumenthal, 1997: Reduced space optimal analysis for historical datasets: 136 yrs of Atlantic sea surface temperatures, J. Geophys. Res. 102, 27,835-27,860.

Linsley, B.K., Wellington, G.M. Schrag, D.P., Ren, L., Salinger, M. and A.W. Tudhope, 2004: Geochemical evidence from corals for changes in the amplitude and spatial pattern of South Pacific interdecadal climate variability over the last 300 years. *Clim. Dynam.*, **22,** 1-11.

Manabe, T., 1999: The digitized Kobe Collection phase I: Historical surface marine meteorological observations in the archive of the Japan Meteorological Agency. *Bull. Am. Met. Soc.,* **80**, 2703-2715.

Minobe S., 1997: A 50–70 year climatic oscillation over the North Pacific and North America. *Geophys. Res. Lett.,* **24**, 683-686.

Minobe, S., 1999: Resonance in bidecadal and pentadecadal climate oscillations over the North Pacific: Role in climatic regime shifts, *Geophys. Res. Lett.,* **26**, 855-858.

Minobe, S., 2000: Spatio-Temporal Structure of the Pentadecadal Variability over the North Pacific. *Prog. in Oceanogr.*, **47**, 381–408.

Minobe, S., 2002: Interannual to interdecadal changes in the Bering Sea and concurrent 1998/99 changes over the North Pacific. *Progr. Oceanogr.,* 55, 45–64.

Mizuno, K., and W. B. White, 1983: Annual and interannual variability in the Kuroshio current system. *J. Phys. Oceanogr.* **13**, 1847-1867.

Nakamura, H., G. Lin, and T. Yamagata, 1997: Decadal climate variability in the North Pacific during the recent decades. *Bull. Am. Met. Soc.*, **98**, 2215-2225.

Nitta, T., and S. Yamada, 1989: Recent warming of tropical sea surface temperature and its relationship to the Northern Hemisphere circulation. *J. Meteor. Soc. Japan,* **67***,* 375-383.

Parker,D. E., C. K. Folland and M. Jackson, 1995: Marine surface temperature: Observed variations and data requirements. *Climatic Change*, **31**, 559-600.

Palmer, T. and Z. Sun, 1985: A modeling and observational study of the relationship between sea surface temperature in the north west Atlantic and atmospheric general circulation. *Q. J. Roy. Met. Soc.*, **111**, 947-975.

Ratcliffe, R.A.S. and R. Murray, 1970: New lag associations between north Atlantic sea temperatures and European pressure, applied to long-range weather forecasting. *Q. J .Roy. Met. Soc.*, **96**, 226-246.

Rayner, N. A., D. E. Parker, E. B. Horton, C. K. Folland, L. V. Alexander, and D. P. Rowell, E. C. Kent, and A.

Kaplan, 2003: Global analyses of sea surface temperature, sea ice, and night marine air temperature since the late nineteenth century. Journal of Geophysical Research, Vol. 108, No. D14, 4407, doi:10.1029/2002JD002670.

Reynolds R. W., and T. M. Smith, 1994: Improved global sea-surface temperature analyses using optimum interpolation. *J. Climate*, **7**, 929-948.

Schneider N, A. J. Miller, D. W. Pierce, 2002: Anatomy of North Pacific decadal variability. *J. Climate*, **15**, 586-605.

Seager, R., Y. Kushnir, N. H. Naik, M. A. Cane, and J. Miller, 2001: Wind-Driven shifts in the latitude of the Kuroshio-Oyashio extension and generation of SST anomalies on decadal timescales. *J. Climate*, **14**, 4249-4265.

Smith T. M, and R. W. Reynolds, 2004: Improved extended reconstruction of SST (1854-1997). *J. Climate*, **17**, 2466-2477.

Tanimoto Y., H. Nakamura, T. Kagimoto, S. Yamane, 2003: An active role of extratropical sea surface temperature anomalies in determining anomalous turbulent heat flux. *J. Geophys. Res.*, **108 (C10)**, 3304, doi:10.1029/2002JC001750.

Trenberth, K. E., 1990: Recent observed interdecadal climate changes in the Northern Hemisphere. *Bull. Am. Met. Soc*., **71***,* 988-993.

Trenberth, K. E., and D. A. Paolino, 1980: The Northern Hemisphere sea-level pressure data set: Trends, errors, and discontinuities. *Mon. Wea. Rev.* **108***,* 855-872.

Woodruff, S. D., R. J. Slutz, R. L. Jenne, and P. M. Steurer, 1987: A comprehensive ocean-atmosphere data set. *Bull. Amer. Meteor. Soc.*, **68**, 1239-1250.

Worley, S. J., S. D. Woodruff, R. W. Reynolds, S. J. Lubker, and N. Lott, 2005: ICOADS Release 2.1 data and products. submitted to *Int. J. Climatol.*

Wu, P. and Rodwell, M., 2003: Gulf Stream forcing of the winter North Atlantic Oscillation. *Atmos. Sci. Lett.*, 5, 57-64, doi:10.1016/j.atmoscilet.2003.12.002.

Yamamoto, R., Iwashima, T. Sanga, N. K. and Hoshiai, M. 1986. An analysis of climate jump. *J. Meteorol. Soc. Japan*, **64**, 273-281.

Zhang Y., J. M. Wallace, and D. S. Battisti, 1997: ENSO-like interdecadal variability: 1900-1993. *J. Climate,* **10***,* 1004-1020.

Table 1. Subjectively removed SST data. The last row indicates that the non-bucket observations (engine intake or unknown) of deck number 705, 706, and 707 were removed.

| regions | lat. | lon. | yr. | SST | deck no. |
|---|---|---|---|---|---|
| central North Pacific | 40°N–45°N | 175°W–170°W & 165°W–160°W | 1850–1975 | All | 732 |
| eastern North Pacific | 26°N–30°N | 125°W–119°W | 1960–1975 | All | 732 |
| tropics | 20°S–20°N | All | All | <3 | All |
| tropics | 20°S–20°N | All | All | <5.5 | 555 706 714 732 883 888 889 892 926 927 |
| western tropical South Pacific | 20°S–Eq. | 140°E–175°W | All | <10 | 714 732 888 892 926 |
| east of Madagascar | 30°S–20°S | 50°E–60°E | All | <5.0 | All |
| eastern tropical South Pacific | 25°S–10°S | 100°W–80°W | All | <5.5 | All |
| east of southern South America | 50°S–40°S | 60°W–50°W | All | All | 732 |
| west of southern South America | 33°S–30°S | 10°E–15°E | All | All | 732 |
| global | All | All | 1939-1941 | non-bucket | 705, 706, 707 |

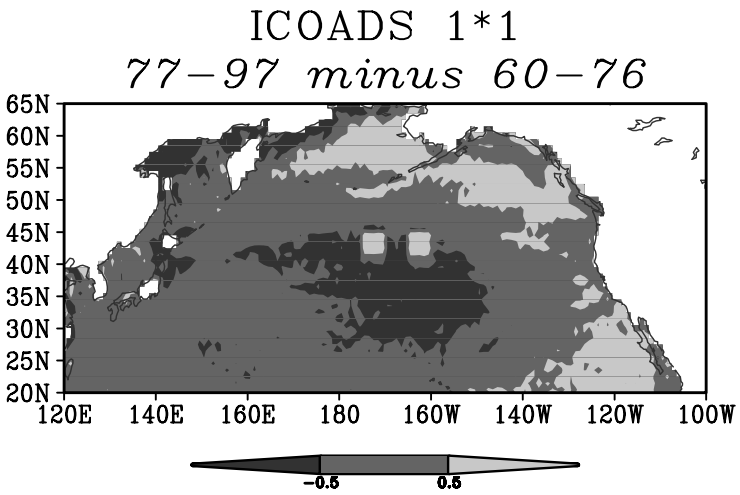


Fig. 1. SST difference between 1977–1997 and 1960–1976 based on gridded ICOADS SSTs on 1°×1° grid. The SST difference is consistent with the PDO pattern shown by Mantua et al. (1997), except for the couple of unrealistic squares (40°N–45°N, 175°W–170°W and 165°W–160°W) in the central North Pacific.

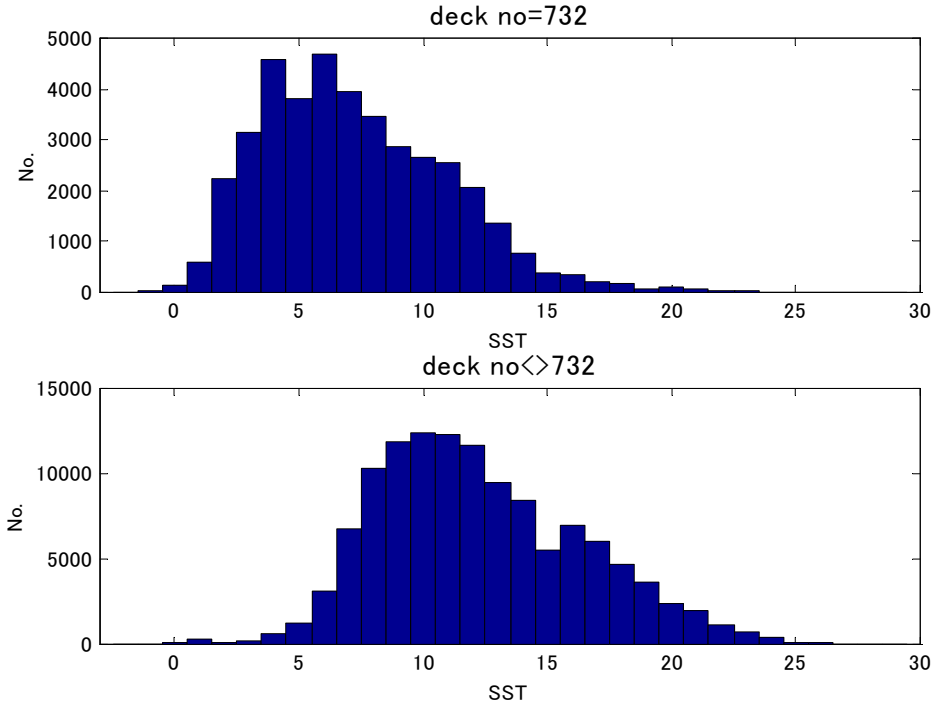


Fig. 2. Histogram of SST data of deck number 732 (upper panel) and SST data of the other deck numbers (lower panel) over 40°–45°N, 175°–170°W and 165°–160°W. The period is 1956–1976 for deck number 732 and 1900–1976 for other deck number. There is no observation before 1956 for the deck number 732 in this region.

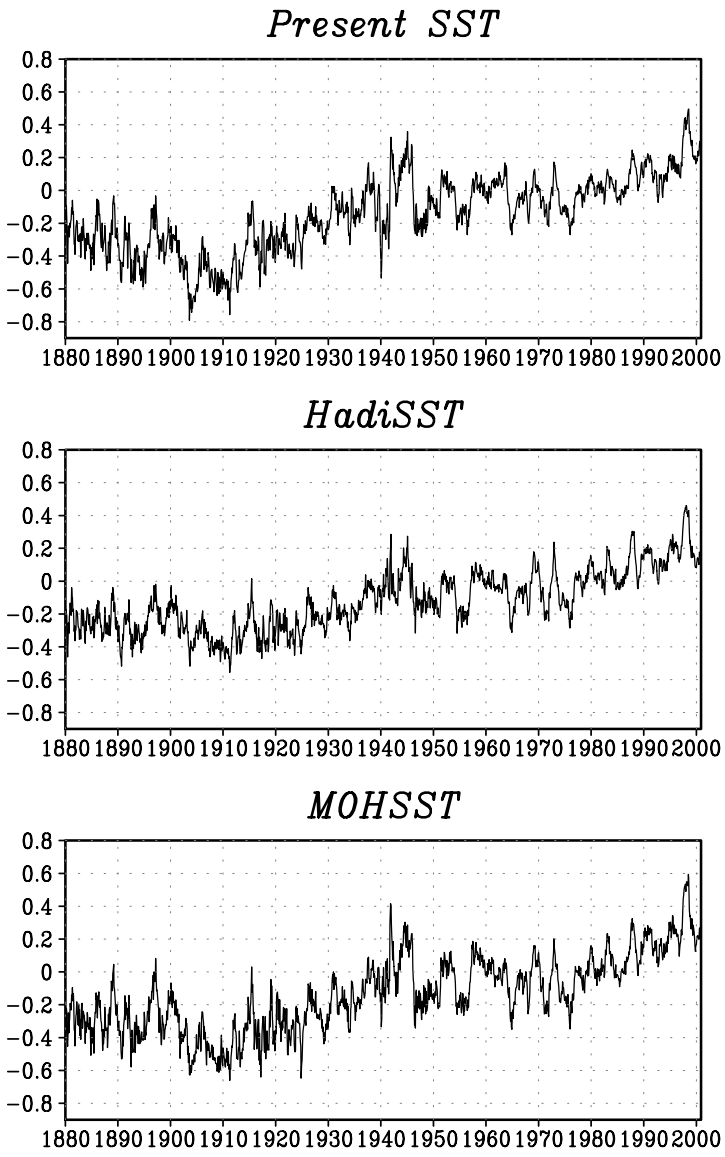


Fig. 3. Global average of monthly SST anomalies relative to 1960–1990 climatology using the present SST (HUSST, top), HadiSST (middle), and MOHSST (bottom).

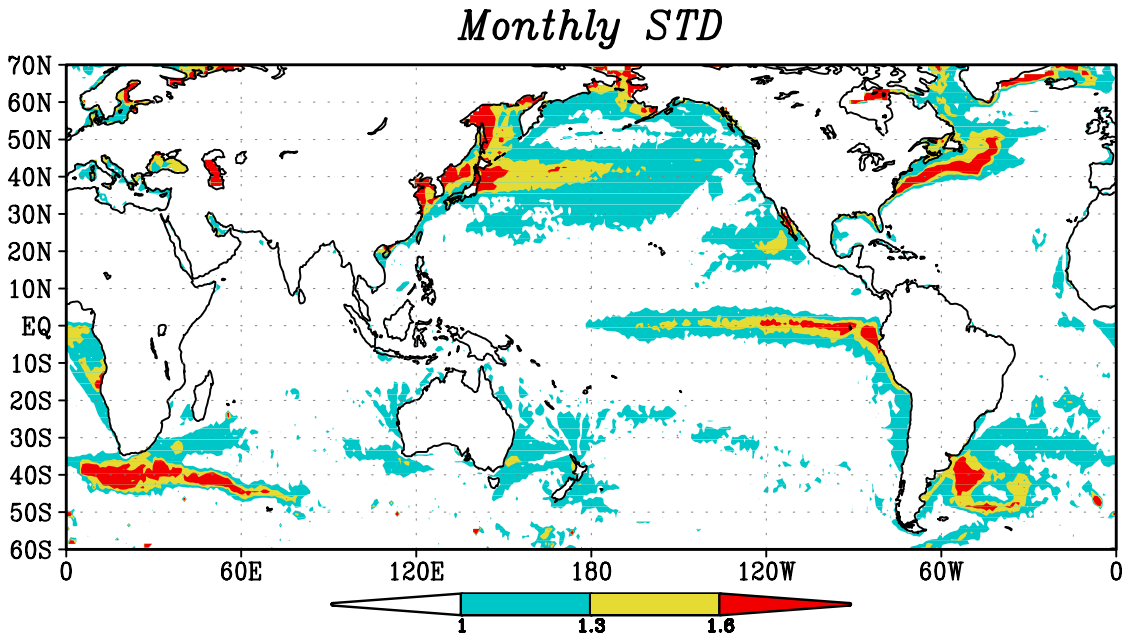


Fig. 4. Standard deviation of monthly SST anomalies during the 20th century (1901–2000). The color scale bar shows shading convention in units of °C.

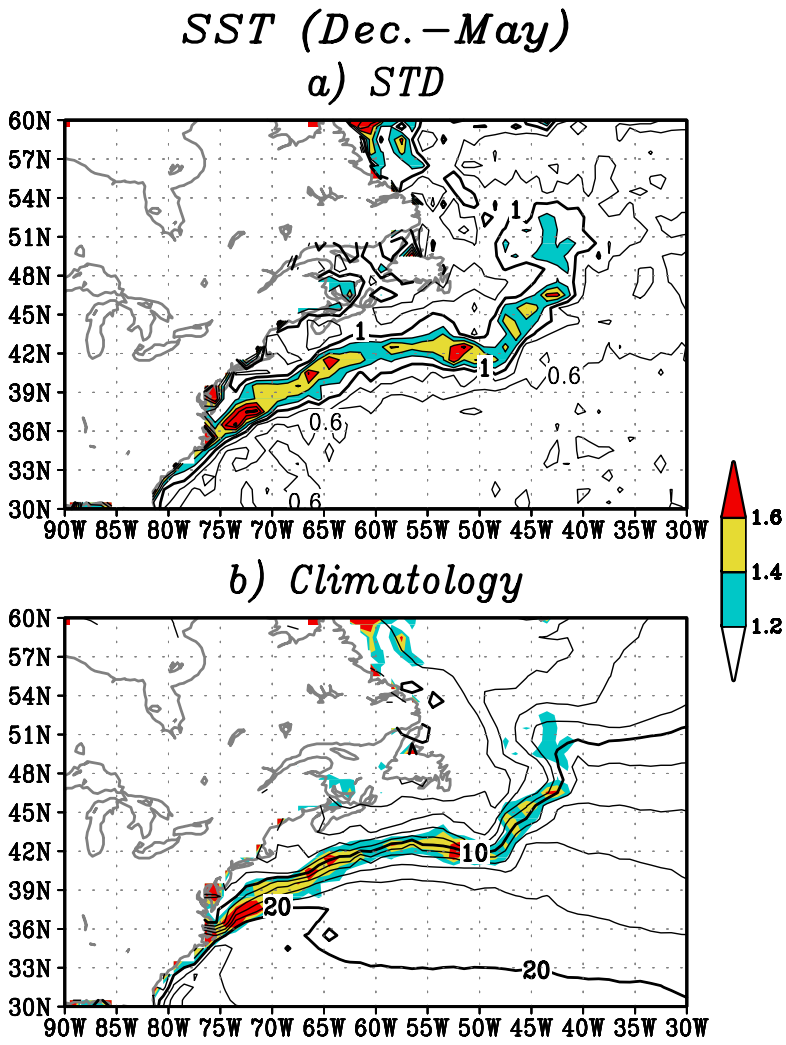


Fig. 5. (a) Standard deviation of SST anomalies averaged over December–May (winter–spring) during the 20th century using the present SST data. Contour interval is 0.2°C with thick contours of 1°C and 2°C, and the color scale bar shows shading convention. The SST anomalies at grids where standard deviations are larger than 1.3°C to the east of 75°W south of 48°N except for coastal grids are used for calculation of the time series of GSE mean SST anomaly shown in Fig. 6. (b) Climatological SSTs for December–May with the same shading of the standard deviations as the top panel.

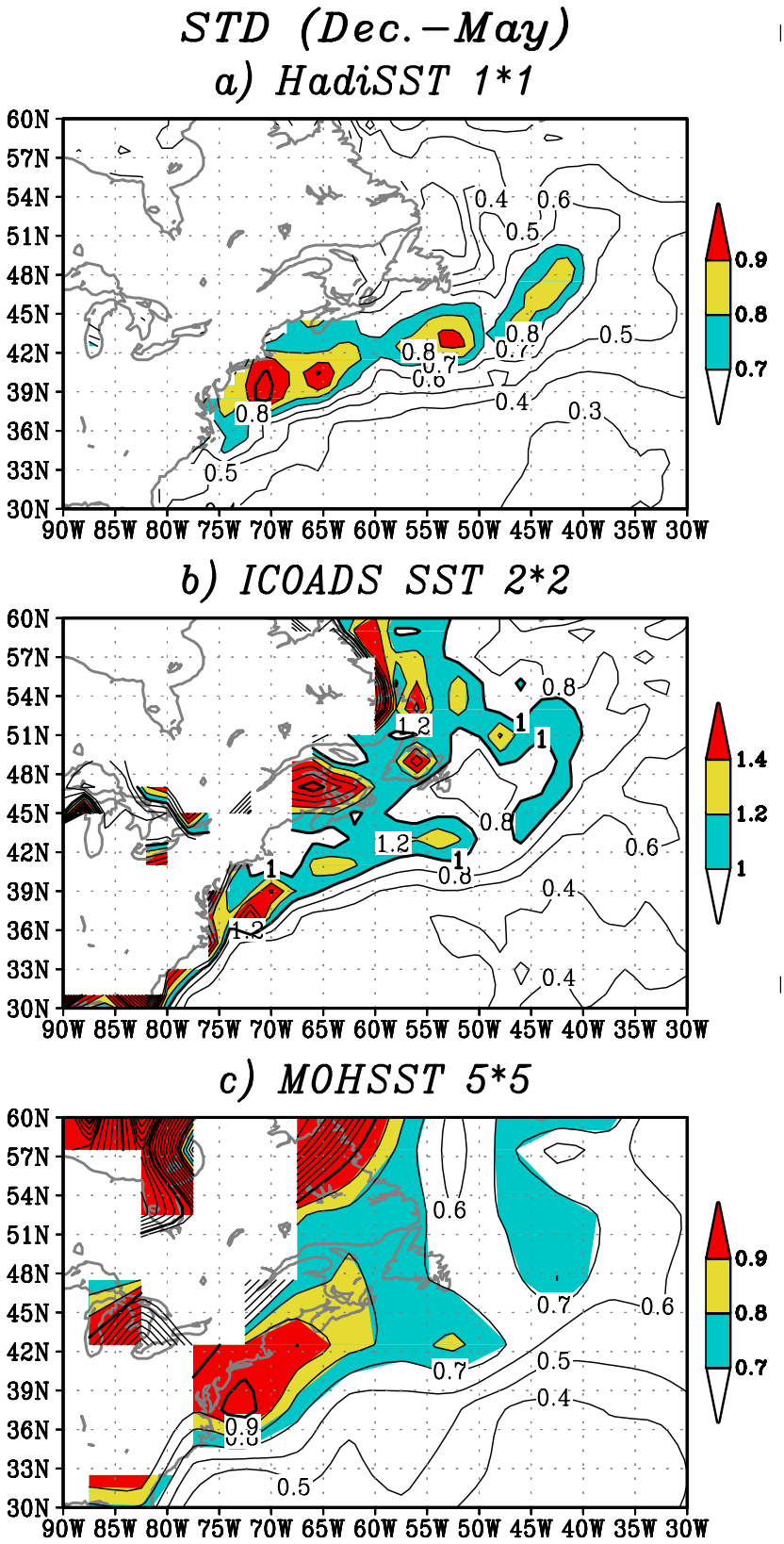


Fig. 6. Same as Fig. 4b, but for (a) HadISST (1°×1° grid), (b) ICOADS SST (2°×2° grid), and (c) MOHSST (5°×5° grid). The contour intervals are 0.1°C for panels (a) and (c), but 0.2°C for panel (b). Shading convention is shown by the color scale bars.

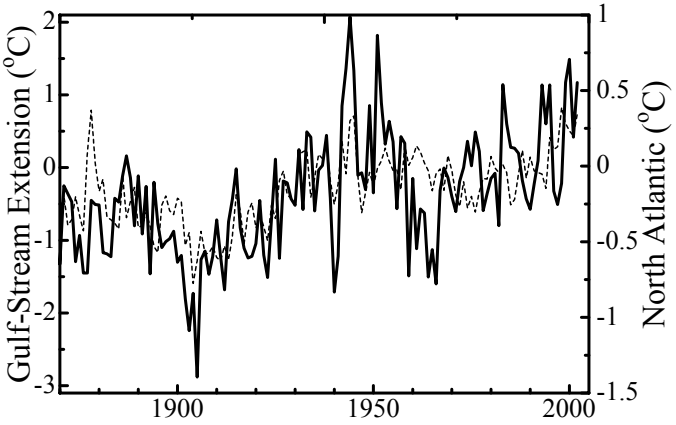


Fig. 7. Winter-spring (December–May) averaged Gulf-Stream Extension SST anomalies (solid line, left axis) along with the North Atlantic mean SST anomalies (dashed line, right axis). Without any smoothing, multidecadal variability is prominent.

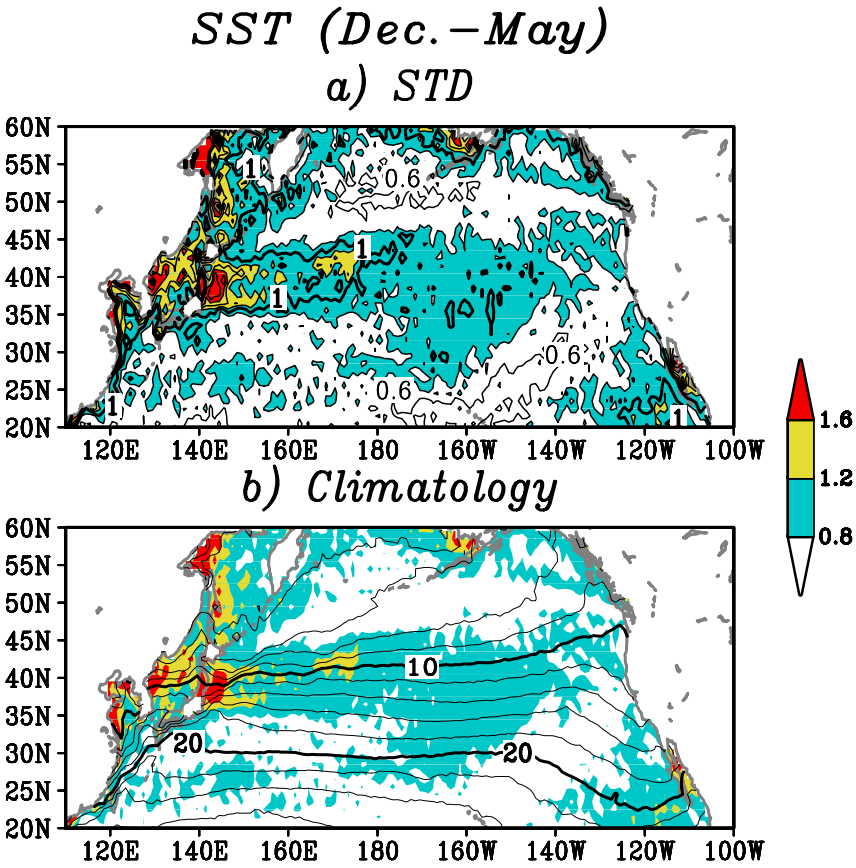


Fig. 8. Same as Fig. 5, but for the North Pacific.

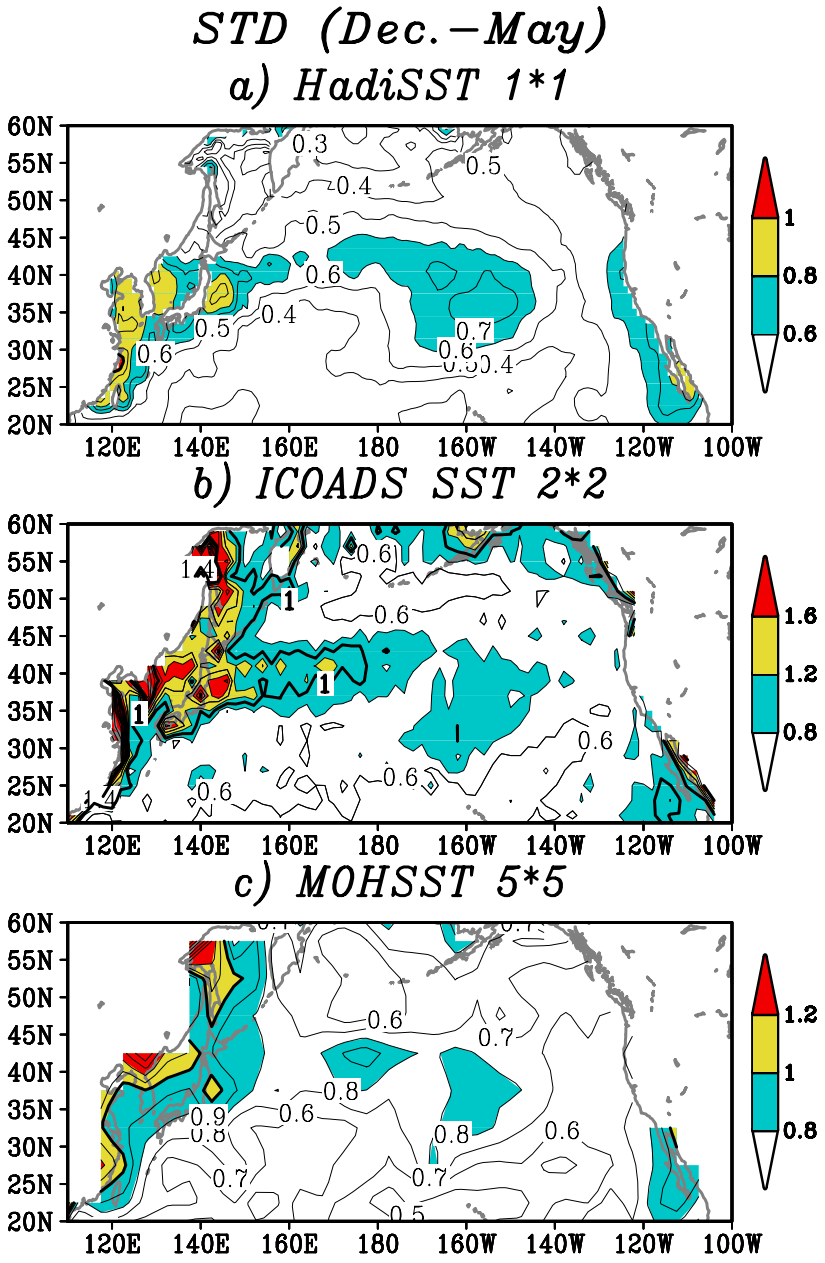


Fig. 9. Same as Fig. 6, but for the North Pacific.

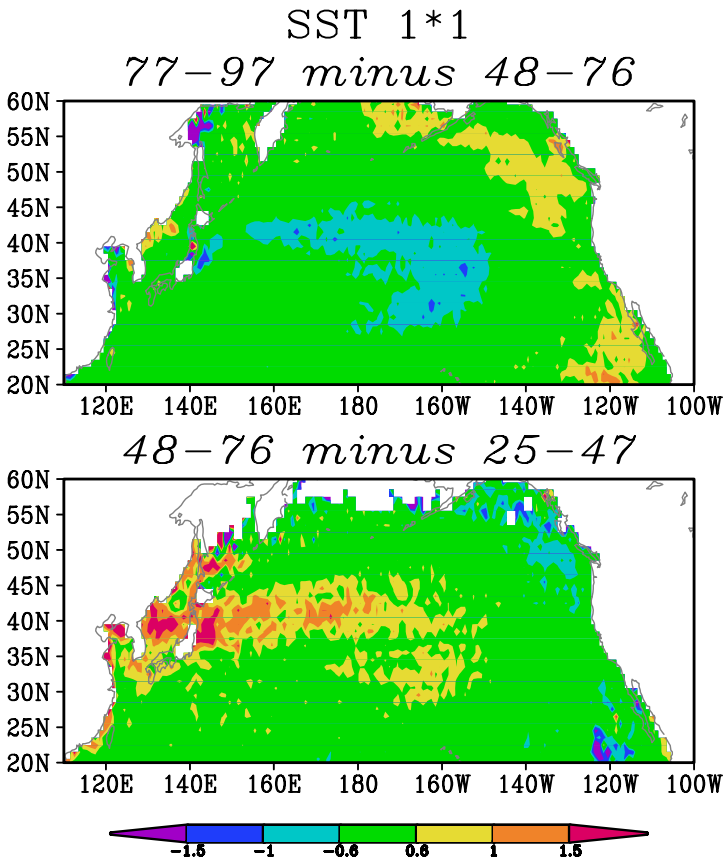


Fig. 10. Winter-spring SST anomaly differences between successive two epochs of a regime associated with the 1970s (top panels) and 1940s (bottom panels) climatic regime shifts. The SST difference is calculated between 1977–1997 and 1948–1976 for the upper panel, and 1948–1976 minus 1925–1947 for the lower panel.

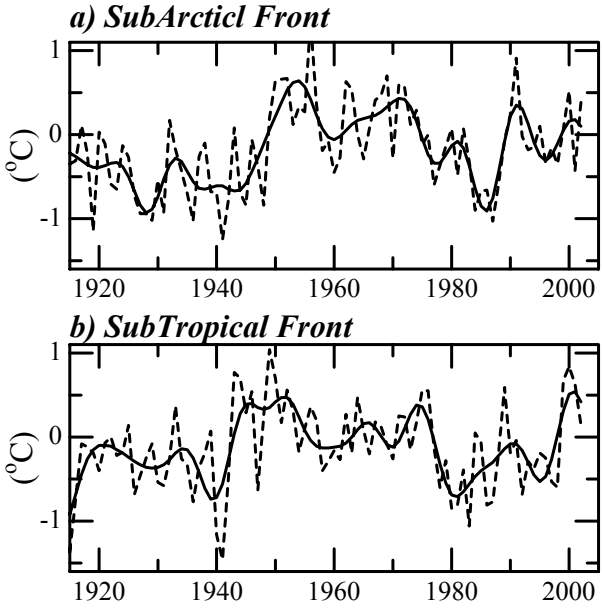


Fig. 11. Time series of SST anomalies (a) for SubArctic Front (SAF) (36°–44°N, 140°E–175°W) and (b) for SubTropical Front (STF) (28°–35°N, 180°–160°W). Dashed lines denote raw anomalies, while solid curves indicate 7-yr low-pass filtered data.